

displacement at the wing trailing edge for various vortex heights. Here again, the present theory produces reasonable estimates. As is anticipated, however, a potential vortex model overpredicts the vortex effect in a very close encounter of vortex and wing due to its singularity at the center. This is evident in the figure by the deviation of the curve from the squares for h/c less than about 0.1. This situation may be improved by modeling a finite vortex core.

Overall, the results are very encouraging, and this suggests that the present method may be used as a preprocessor to prescribe the vortex path over a lifting surface for vortex-lifting surface interaction calculations within the restrictions of the potential flow assumptions. This will eliminate the need to assume a straight vortex and update the whole flow field as well as the vortex path. Or, in cases where complex configurations are involved, the present method may provide a reasonable starting position of the vortex for a coupled iteration scheme.

Acknowledgment

A portion of the work was performed under Army Research Office Contract DAAG 29-84-K-0131, Experimental Simulation of Transonic Vortex-Airfoil Interactions.

References

- ¹Hancock, G. J., "Aerodynamic Loading Induced on a Two-Dimensional Wing by a Free Vortex in Incompressible Flow," *The Aeronautical Journal of the Royal Aeronautical Society*, Vol. 75, June 1971, pp. 413-416.
- ²Patel, M. H. and Hancock, G. J., "Some Experimental Results of the Effect of a Streamwise Vortex on a Two-Dimensional Wing," *Aeronautical Journal*, April 1974, pp. 151-155.
- ³Harvey, J. K. and Perry, F. J., "Flowfield Produced by Trailing Vortices in the Vicinity of the Ground," *AIAA Journal*, Vol. 9, Aug. 1971, pp. 1659-1660.
- ⁴Seath, D. D. and Wilson, D. R., "Vortex-Airfoil Interaction Tests," AIAA Paper 86-0354, Jan. 1986.
- ⁵Maskew, B., "Predicting Aerodynamic Characteristics of Vortical Flows on Three-Dimensional Configurations Using a Surface-Singularity Panel Method," AGARD-CP-342, 1983.
- ⁶Steinhoff, J., Ramachandran, K., and Suryanarayanan, K., "The Treatment of Convected Vortices in Compressible Potential Flow," AGARD-CP-342, April 1983.
- ⁷Karamcheti, K., *Principles of Ideal-Fluid Aerodynamics*, John Wiley, New York, 1966, Chap. 19, pp. 538-545.
- ⁸Bisplinghoff, R. L., Ashley, H., and Halfman, R. L., *Aeroelasticity*, Addison-Wesley, Reading, Mass., 1955, Chap. 5, pp. 231-237.

Divergence Study of a High-Aspect-Ratio, Forward Swept Wing

Stanley R. Cole*

NASA Langley Research Center, Hampton, Virginia

Introduction

THE present study was conducted to obtain data that could be used to assess the prediction capabilities of a currently available aeroelastic code for a high-aspect-ratio, forward-swept wing. A wind tunnel experiment was conducted in the NASA Langley Transonic Dynamics Tunnel (TDT) on a model with a panel aspect ratio of 9.16 (unswept). Aeroelastic analyses were conducted for each condition tested in the TDT

Presented as Paper 86-0009 at the AIAA 24th Aerospace Sciences Meeting, Reno, NV, Jan. 6-9, 1986; received Feb. 2, 1986; revision received Nov. 23, 1987. Copyright © 1986 American Institute of Aeronautics and Astronautics, Inc. No copyright is asserted in the United States under Title 17, U.S. Code. The U.S. Government has a royalty-free license to exercise all rights under the copyright claimed herein for Governmental purposes. All other rights are reserved by the copyright owner.

*Aerospace Technologist, Configuration Aeroelasticity Branch, Senior Member AIAA.

for this comparison. The wind tunnel model was tested at various forward sweep angles. A rectangular tip shape was used during most of the experiment. A tip parallel to the flow in the 45 deg forward-sweep position was also tested for further correlation with analysis. General aeroelastic characteristics of the high-aspect-ratio, highly swept wing, and the prediction capabilities of the analysis code are discussed in this Note.

Test Apparatus and Procedures

The model used in this study was untapered, had a 4.51 ft semispan and a semispan aspect ratio of 9.16 in the unswept position. The airfoil section was a NACA 0014. The model wing was constructed of a layered fiberglass shell, which provided both structural stiffness and the airfoil shape, with a rectangular aluminum spar located at the 30% chord position to increase the bending stiffness. Semicircular wing tips made of balsa wood were used to improve the flow over what would otherwise have been a blunt wing tip in the forward-sweep positions. The model was clamped in a cantilevered manner to the wind-tunnel sidewall.

The model was positioned manually to sweep angles Λ of 0, -15, -30, -45 and -60 deg. A composite photograph showing the model in the various sweep angles is shown in Fig. 1. The model was tested with a rectangular wing tip at each azimuth angle as shown in the figure. In addition, the wing tip was modified such that the tip was parallel to the freestream flow when tested in the $\Lambda = -45$ deg position. The two tip shapes are shown in Fig. 1 at $\Lambda = -45$ deg.

Experimental predictions of static aeroelastic divergence were made using subcritical response techniques.¹ For each sweep angle tested, subcritical data were taken at gradually increasing values of dynamic pressure. At each dynamic pressure q , the model angle of attack was first adjusted to a 1-g lift condition so that the weight of the model was aerodynamically supported. The angle of attack was then incrementally increased and the root bending moment M_e was measured at each angle of attack α . Typical data obtained for the subcritical response divergence predictions are shown in Fig. 2. These data were used to predict the dynamic pressure at which divergence would occur. Two subcritical response techniques, an improved static Southwell method and the divergence index method, were used during this test. Reference 1 discusses these prediction methods in greater detail.

Analytical Tools

Aeroelastic analyses were conducted for the wind-tunnel model to determine the validity of the analysis code for a high-aspect-ratio, highly swept wing. A vibration analysis was performed with the finite-element method program² Engineering Analysis Language (EAL). General beam elements were utilized to assemble the finite-element model. Elements were ar-

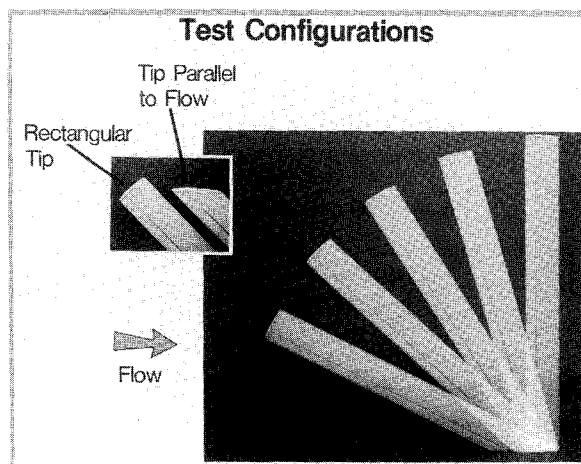


Fig. 1. Composite photograph showing each sweep angle tested and the two tip shapes tested in the $\Lambda = -45$ deg configuration.

ranged to simulate the stiffness properties along the measured elastic axis of the model. Stiffness properties derived from laboratory measurements were used for the beam elements. Lumped masses were located to simulate the chordwise center of gravity position of the model. These lumped masses were offset from the structural elastic axis by very stiff beam elements to virtually eliminate any chordwise warpage of the analytical model. Additional elements (with no mass) were located at the leading and trailing edges to obtain displacements around the perimeter of the model for use in the aeroelastic analysis. Natural frequencies, natural mode shapes, and generalized masses were calculated using EAL.

A flutter analysis software system, known as FAST³, was used to predict the aeroelastic instabilities of the model. FAST calculates planar subsonic kernel function lifting-surface aerodynamics based on the natural mode shapes, natural frequencies, and generalized masses (as calculated through EAL) for the wing being analyzed. Four primary natural vibration modes were used in the present analysis. An aeroelastic instability solution is then completed by FAST with these calculated aerodynamics using the k method.⁴ Divergence calculations are made by FAST provided the aerodynamics are calculated for a reduced frequency of zero.

Aeroelastic calculations were made for the various sweep angles by varying the sweep of the analytical lifting surface. The planforms used in the analysis for the various sweep positions corresponded to the appropriate portion of the experimental model exposed to the flow. The structure was identical in all the sweep angles. Thus, the simulated structure of the model was identical for all of the sweep configurations. In addition, the structure was considered to remain the same for the two wing tip shapes. The wing tips were modeled analytically by changing the planform geometry to account for the aerodynamic changes induced by the wing tip shapes. The analytical wing tip shapes correspond to the geometry shown in Fig. 1.

Results and Discussion

Divergence measurements were made during the TDT wind-tunnel test at Mach number $M = 0.4$ for sweep angles of 0, -15, -30, -45, and -60 deg with the rectangular tip shape. A tip parallel to the flow was tested only in the $\Lambda = -45$ deg position. The experimental results shown in Fig. 3 show the dramatic decrease in divergence dynamic pressure q that occurred even at small forward sweep angles compared to the unswept wing and that the most critical configuration was at $\Lambda = -45$ deg.

The effect of the two tip shapes tested is also shown in Fig. 3. The tip parallel to the flow increased the divergence dynamic pressure by 14% compared to the rectangular tip at $\Lambda = -45$ deg. Tip effects similar to these have been documented previously for much lower aspect ratio wings.⁵ These two tips are identical in the unswept position, so the effect of the tip may be progressively less as the sweep angle is decreased from $\Lambda = -45$ to $\Lambda = 0$ deg.

The FAST aeroelastic software system was used to calculate divergence conditions for the model in each sweep configuration. Four natural modes were used in the analysis. These modes were the three lowest frequency vertical (flapwise) bending modes and the first torsion mode. Analysis also was made for the parallel tip shape in the $\Lambda = -45$ deg configuration. The tip shape was modeled in the analysis by adjusting the planform geometry so that the tip was either rectangular with respect to the wing planform geometry or parallel with the freestream flow direction. The correlation between experiment and analysis at $M = 0.4$ can be seen in Fig. 3. The analysis was conservative at all forward sweep angles. At $\Lambda = -45$ deg, the analysis was 14% conservative. In the unswept position, analysis matched the experimental results. The effect of the two tip shapes tested at $\Lambda = -40$ deg was predicted accurately by analysis. Divergence was the critical instability at all sweep angles, although flutter was analytically predicted to oc-

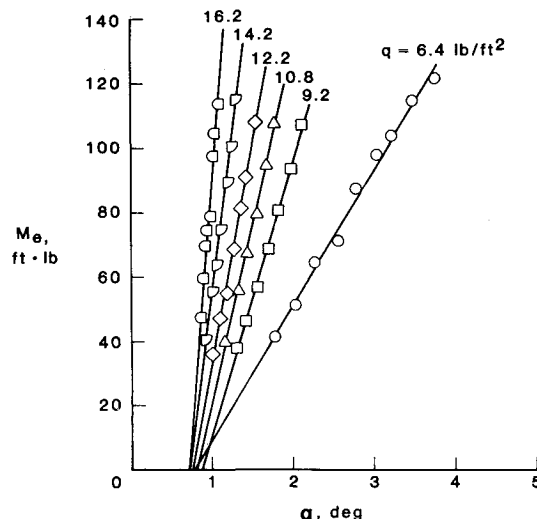


Fig. 2. Typical data obtained for subcritical response divergence predictions. $\Lambda = -45$ deg, $M = 0.4$.

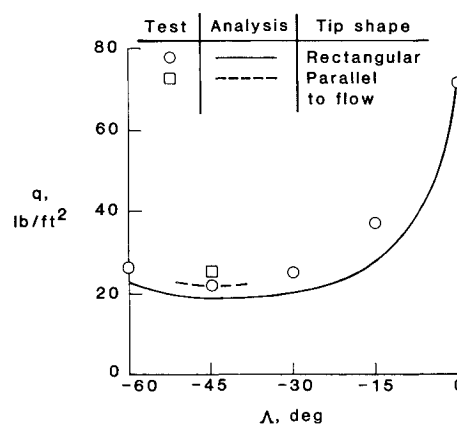


Fig. 3. Divergence boundaries for both tip models compared with calculated boundaries.

cur at nearly the same dynamic pressure as divergence at $\Lambda = 0$ deg. This predicted flutter condition is primarily a coupling of the second vertical (flapwise) bending mode and the first torsion mode. Similar flutter results have been shown to occur in other forward-swept wing experiments (see Ref. 1). In some instances, flutter is actually the critical instability at small forward sweep angles (-15 deg $< \Lambda < 0$ deg). This was not the case for the high-aspect-ratio wing tested in this experiment. For this model, as the sweep angle was decreased, the predicted flutter condition rapidly moved to higher velocities (higher dynamic pressures).

Conclusions

A study of static aeroelastic divergence has been conducted for a high-aspect-ratio, forward-swept wing model. Divergence characteristics were determined experimentally and analytically at sweep angles of 0, -15, -30, -45, and -60 deg. A rectangular tip shape was tested at all sweep angles. In addition, for $\Lambda = -45$ deg, a tip parallel to the flow was tested.

The wing tip shape had a significant effect on the divergence phenomenon. For $\Lambda = -45$ deg, a wing tip parallel to the flow increased the divergence dynamic pressure by 14% compared to a rectangular wing tip.

The analytical predictions using subsonic lifting surface theory were conservative. At $\Lambda = -45$ deg, the analysis predicted a divergence dynamic pressure 14% lower than the experimental value.

References

¹Ricketts, R.H. and Doggett, R.V., Jr., "Wind-Tunnel Experiments on Divergence of Forward-Swept Wings," NASA TP-1685, 1980.

²Whetstone, W.D., *EISI-EAL Engineering Analysis Reference Manual*, Engineering Information Systems, Inc., 1983.

³Desmarais, R.N. and Bennett, R.M., "User's Guide for a

Modular Flutter Analysis Software System (FAST Verion 1.0)," NASA TM-78720, 1978.

⁴Desmarais, R.N. and Bennett, R.M., "An Automated Procedure for Computing Flutter Eigenvalues," *Journal of Aircraft*, Vol. 11, Feb. 1974, pp. 75-80.

⁵Diederich, F.W. and Budiansky, B., "Divergence of Swept Wings," NACA TN-1680, 1948.

Errata

In-Flight Flow Visualization of F-106B Leading-Edge Vortex Using the Vapor-Screen Technique

J. E. Lamar,* R. A. Bruce,†

J. D. Pride Jr.,‡ R. H. Smith,§ and P. W. Brown¶
NASA Langley Research Center, Hampton, Virginia
and

T. D. Johnson Jr.**
PRC Kentron, Inc., Hampton, Virginia

[JA 25, pp. 113-120 (1988)]

THE following errors were made during the production of this paper:

Figure 10 should have been printed as it appears here:

Reference five should appear as follows:

⁵Fennell, L. J., "Vortex Breakdown—Some Observations in Flight on the HP 115 Aircraft," British A.R.C., U.K., R&M No. 3805, 1977.

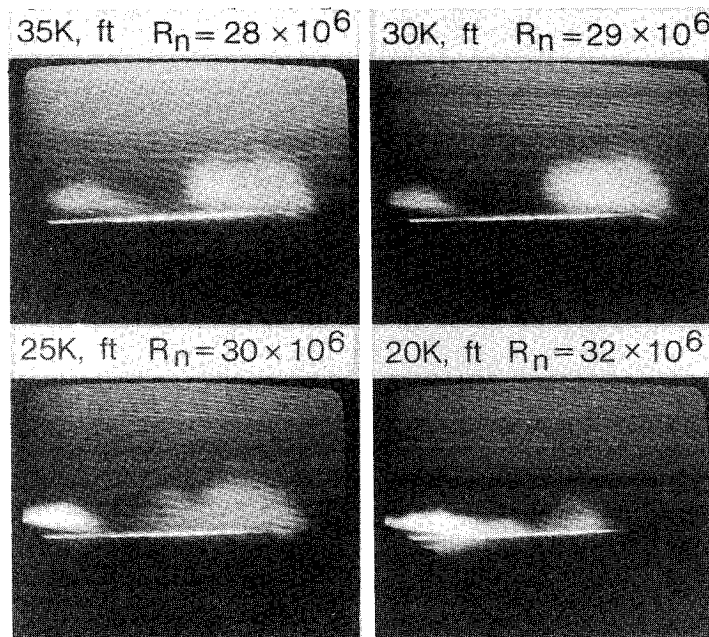


Fig. 10 Effect of Reynolds number on vortex system; $\alpha \sim 18$ deg, $\sim 1 = g$, probe #6, slit width = 0.041 in.

The AIAA editorial staff regrets these errors and apologizes for any inconvenience.

Notice to Subscribers

We apologize that this issue was mailed to you late. As you may know, AIAA recently relocated its headquarters staff from New York, N.Y. to Washington, D.C., and this has caused some unavoidable disruption of staff operations. We will be able to make up some of the lost time each month and should be back to our normal schedule, with larger issues, in just a few months. In the meanwhile, we appreciate your patience.